17th World Conference on Earthquake Engineering, 17WCEE
Sendai, Japan - September 13th to 18th 2020

EXPERIMENTAL INVESTIGATION AND CAPACITY EVALUATION OF FERRO-CEMENT LAMINATED MASONRY INFILLED RC FRAME

D. Sen[(1)], H. Alwashali[(2)], Z. Tafheem[(3)], M.S. Islam[(4)], M. Maeda[(5)], M. Seki[(6)]

[(1)] *Ph.D. student, Tohoku University, Japan, dsendip@rcl.archi.tohoku.ac.jp*
[(2)] *Assistant Professor, Tohoku University, Japan, hamood@rcl.archi.tohoku.ac.jp*
[(3)] *Ph.D. student, Tohoku University, Japan, zasiah@rcl.archi.tohoku.ac.jp*
[(4)] *Post-doctoral Researcher, Tohoku University, Japan, shafiul@rcl.archi.tohoku.ac.jp*
[(5)] *Professor, Tohoku University, Japan, maeda@rcl.archi.tohoku.ac.jp*
[(6)] *Research Fellow, Building Research Institute, Japan, sekimatsutaro@yahoo.co.jp*

Abstract

Recent earthquakes in developing countries demonstrated the deficiency of lateral resistance of RC buildings which sparks the necessity of strengthening of existing RC buildings. Generally, masonry wall as partition walls within RC frame is very common construction practice in developing countries which sometimes improve the lateral strength. However, additional strengthening measure on masonry infilled RC building is required to save the buildings by improving lateral strength up to the seismic demand. Strengthening of masonry infill with mesh reinforcement (e.g. polypropylene band, steel wire mesh, textile fiber) embedded in a cementitious overlay is one of the existing strengthening techniques. Among several overlay techniques, steel wire mesh embedded mortar i.e. ferro-cement lamination might be a potential candidate for developing countries as it is an easy to apply method. Ferro-cement refers to steel wire mesh embedded in a mortar overlay, where mesh reinforcement is attached to the masonry infill wall and/or RC frame by means of anchorage. Ferro-cement has been used as a construction and repair material for decades; however, there is still no design guideline for retrofitting of infilled masonry and also the application of ferro-cement on infilled masonry has not been well established in building codes. The main reason is that the failure modes and strength enhancement has not been comprehensively evaluated. Several researchers studied ferro-cement strengthening with a view to improve lateral strength and ductility, however, the effect on the surrounding frame and the global failure modes has been overlooked. In other words, the application of ferro-cement is still done as non-engineered strengthening scheme with no strong background for the evaluation of its' influence on seismic capacity.

This study presents experimental results of two ferro-cement strengthened specimens, with low and high mesh reinforcement content. The first objective is to investigate the effect of wire mesh ratio of ferro-cement on overall structural behavior, i.e. strength and failure mode of ferro-cement laminated masonry infilled RC frame. The second objective is to clarify all possible failure modes after ferro-cement strengthening of infill masonry based on current and past studies. Following this, lateral strength evaluation of three failure modes; *i*) flexural yielding of RC frame, *ii*) joint failure and column punching and *iii*) diagonal compression failure, have been discussed. The experimental results showed that in both cases of strengthening of infilled masonry, i.e. low and high mesh reinforcement ratio, failure mode was flexural yielding of RC frame which is not identified in past studies. Since the failure modes governed by flexure, therefore wire mesh ratio did not affect the lateral strength much. In addition, the lateral strength capacity evaluation of ferro-cement laminated masonry infilled RC frame has been conducted for three failure mechanisms, as mentioned earlier, with fair agreement with experimental results of this study and literature.

Keywords: Ferro-cement; Wire mesh; Laminated masonry infill; Seismic strengthening; Masonry infilled RC frame

1. Introduction

Seismic strengthening of vulnerable RC buildings is one of the most important concern for structural engineers, especially in developing countries, because of the severe damages and large number of injuries occurred during past earthquakes, such as Nepal Earthquake 2015. RC buildings with masonry infill are one of the most popular structures in developing countries. Generally, masonry infill walls are used as partition and commonly considered non-structural elements, however infill masonry could improve the lateral strength capacity. In this context, strengthening of existing infill masonry, and utilizing it as structural element would be a feasible and low cost solution. As a low cost strengthening material, several researchers [1-6] used ferro-cement to strengthen masonry infilled RC frame. In general, ferro-cement (FC) retrofitting of masonry refers to the application of an initial mortar layer on the both faces of masonry wall which is followed by the placement of steel wire mesh and a second mortar layer, as shown in Fig.1. Anchorages are also being used to attach wire mesh to masonry and/or RC frame. Though, ferro-cement has been utilized for decades as a construction material, there is no design specification of FC (e.g. amount of mesh reinforcement, mortar thickness) which can be used for shear strengthening of unreinforced infilled masonry. In addition, all of the previous studies [1-4,6] mainly focused on in-plane capacity improvement of relatively low strength infill masonry (masonry compressive strength 6 ~15MPa), rather than focusing on load transfer mechanism i.e. failure mode evaluation. Most of the previous studies, explained failure mode as crushing or shear cracking of FC laminated masonry infill, which is similar to infill masonry. However, the failure of surrounding RC frame might not be exactly similar as masonry infilled RC frame, i.e. formation of flexural hinge, because stiffness and strength of FC laminated infill masonry is much higher than that of infill masonry, which has been completely overlooked.

Considering the aforementioned lack of studies, this study aims to experimentally investigate effect of wire mesh steel area ratio on lateral behaviour, especially failure mechanism and strength, of FC laminated masonry infilled RC frame. In addition, current study also aims to clarify all possible failure modes, and subsequently propose and validate lateral strength capacity evaluation model for three failure modes from experimental program and also past studies.

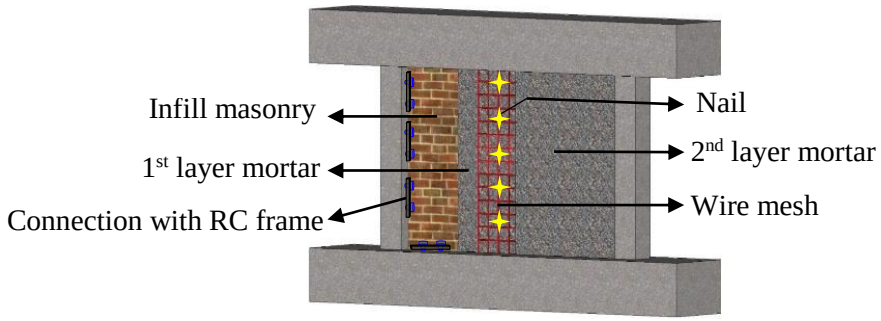

Fig. 1- Schematic diagram of FC lamination on masonry infill

2. Experimental program

2.1 Specimen design concept

In this study, primarily experimental results of several half scaled masonry infilled RC frames, with and without ferro-cement strengthening, have been acquired from literature [1-6] to get an idea about the practices in research field. All the studied FC laminated masonry walls contain square wire mesh on solid or hollow bricks. The lateral contribution of ferro-cement layer has been determined from the difference in lateral capacity of strengthened and un-strengthened specimens. Afterward, the shear stress on FC lamination (τ_{FC}) has been computed considering cross sectional area of FC laminate. The shear stress on laminate is presented in Fig. 2 as a function of normalized horizontal mesh reinforcement area ($\rho_{wm} = A_{hs}/A_{mas}$, where A_{hs} = total cross sectional area of horizontal mesh reinforcement, and A_{mas} = horizontal cross sectional area of masonry (length x thickness)). As shown in Fig. 2, the previous studies had horizontal mesh reinforcement between 0.05~0.35% of the horizontal masonry area. The shear stress on FC layer varied greatly between specimens.

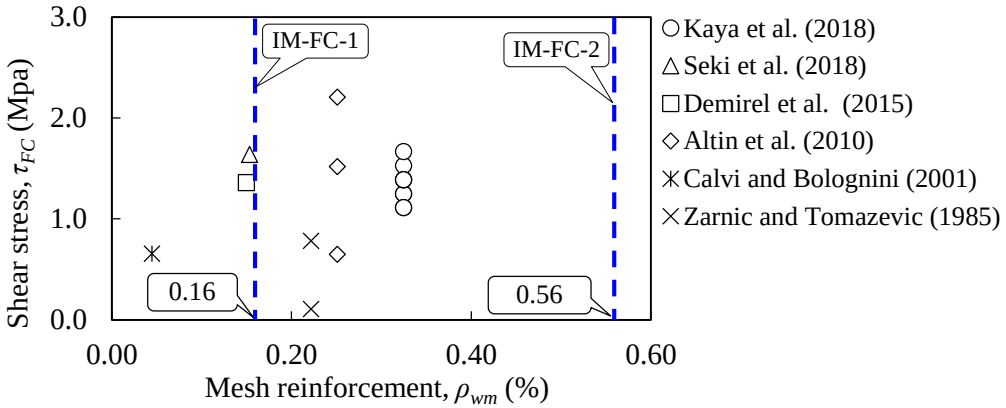

Fig. 2- Shear strength of FC layer as a function of mesh reinforcement ratio

This large variation might be due to variation of failure modes, materials, and connections. In other words, wire mesh might not provide shear strength in a linear manner with the increase of wire mesh, rather it perhaps depends on the interaction between FC laminated infill and surrounding RC frame.

As mentioned earlier, one of the objectives of this study is to investigate the effect of wire mesh ratio on the failure mechanism and strength of FC laminated masonry infilled RC frame. Therefore, wire mesh ratio for current study have been set to 0.16% (relatively low ratio) for specimen IM-FC-1 and 0.56% (relatively high ratio) for specimen IM-FC-2. For specimen IM-FC-2 wire mesh ratio has been set 0.56%, almost 3.5 times than specimen IM-FC-1, to investigate the effect of higher wire mesh ratio on the failure mechanism of surrounding RC frame. It is worthy to note that in this study FC has been applied on relatively strong masonry (masonry compressive strength > 25 MPa) for strengthening purpose to understand the effect on surrounding RC frame's failure.

2.2 Specimen details

Two half scaled masonry infilled RC frames have been constructed and infill masonry has been strengthened with ferro-cement. The overall geometry of RC frame is shown in Fig. 3(a). The details of all the specimens are shown in Table 1. The construction procedure of specimens is as follows: First, RC frame has been constructed and then masonry panel has been built inside the frame, with solid bricks of 210x100x60 mm, in running bond manner. After seven days of masonry construction, 10mm thick mortar has been mounted on the both faces of masonry wall. This is followed by the attachment of square wire mesh to the RC frame and masonry wall. The wire mesh has been connected to surrounding RC frame with bolt (inserted into pre-installed thread) and steel plate as shown in Fig. 3(b). In addition, the wire mesh has been connected with masonry infill by 32mm long nails to hold the wire mesh in place during application of second layer mortar. The nails have been placed in drilled holes at a horizontal and vertical center to center distance of 250mm and 500mm, respectively. After seven days, the second layer of mortar, having 15mm thickness, has been applied on the wire mesh.

2.3 Material properties

The material tests of concrete, reinforcing steel have been conducted for each specimen as per Japanese standard [7]. The wire mesh has been tested as per ACI 549 [8]. The masonry compressive strength has been tested according to ASTM [9]. The mechanical properties of concrete, reinforcing steel, masonry, mortar and wire mesh are shown in Table 2.

2.4 Instrumentation and loading system

Both specimens have been subjected to cyclic lateral loading and 200kN constant vertical loads on each column

to simulate the actual loading on column in buildings. The schematic diagram of the loading system is shown in Fig. 4(a), where two pantographs have been used to avoid any out-of-plane movement of the frame during loading. The cyclic lateral loading program consisted of two cycles for each lateral drift of 0.05, 0.1, 0.2, 0.4, 0.6, 0.8, 1.0, 1.5, and 2.0 %. The lateral drift is defined as the ratio of top lateral displacement, measured at the center of beam, to the height of column taken from the top of foundation stub. The average lateral top displacement has been recorded using LVDTs attached at the center of top beam, as shown in Fig. 4(b). Displacement transducers have also been attached at interval of 220mm over the height RC columns, as shown in Fig. 4(b). Strain gauges have been attached on main reinforcements at interval of 280mm over the height of column. Strain gauges have also been attached on the tie reinforcement at top and bottom of RC column.

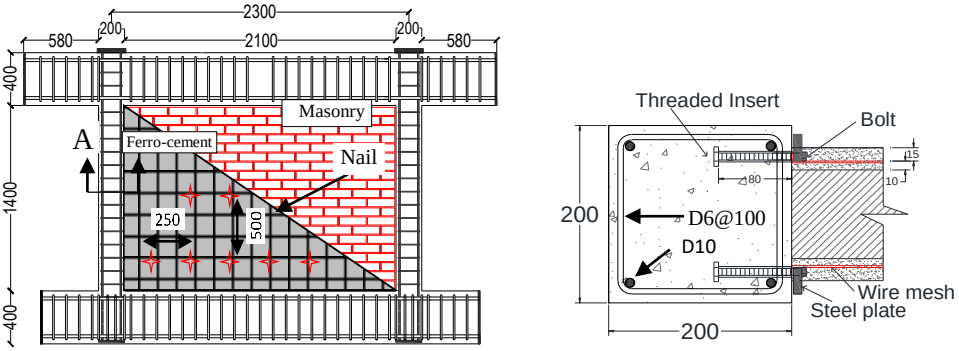

(a) (b) Section A-A

Fig. 3- (a) Geometry of masonry infilled RC frame and (b) connection of wire mesh to RC frame

Table 1- Details of Specimen

Specimen	RC column (mm x mm)	Wire mesh		
		Diameter, φ (mm)	Spacing, s (mm)	Mesh reinforcement, ρ_{wm} (%)
IM-FC-1	200x200	0.9	5.45	0.16
IM-FC-2		1.6	4.75	0.56

Table 2- Material Properties (all values are in MPa)

Specimen	Concrete compressive strength, $f_{c'}$	Reinforcement yield strength, f_y	Masonry		Ferro-cement	
			Compressive strength, f_{mas}	Mortar strength, $f_{mor,j}$	Mortar strength, $f_{mor,FC}$	Wire mesh ultimate strength, $f_{u,wm}$
IM-FC-1	24	350	27	37	26	378
IM-FC-2	26		29	35	29	318

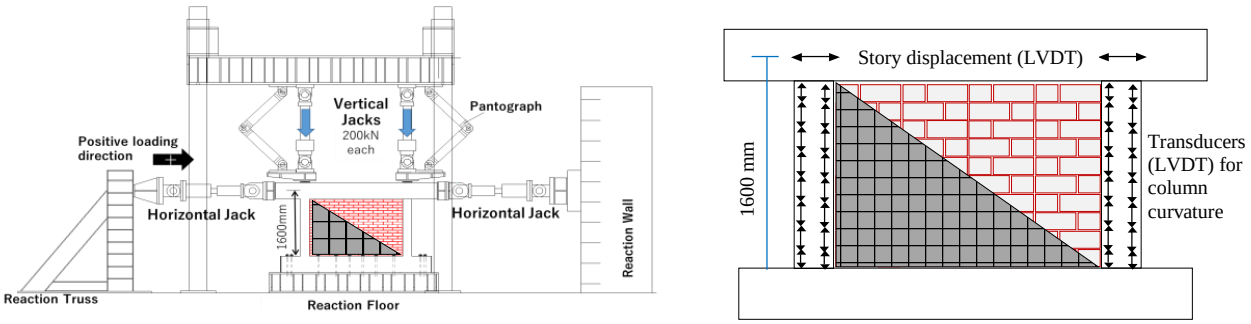

(a) (b)

Fig. 4- (a) schematic diagram of loading system and (b) displacement measurement details

3. Experimental results

3.1 Cyclic lateral behavior and damages

3.1.1 IM-FC-1 (with lower wire mesh ratio i.e. 0.16%)

The hysteresis loops of IM-FC-1 is shown in Fig. 5(a). The response was essentially linear up to the formation of first crack on tension column at 0.05% story drift. At 0.1% story drift, the longitudinal reinforcement yielded at the bottom of tensile column. At 0.2% story drift, flexural crack at the joint of strengthened wall and stub beam, as shown in Fig. 6(a), has also been observed. After cracking, the hysteresis loops began to wide, specifically at the cycle of 0.4% story drift in which specimen reached to its maximum capacity and inclined crack appeared on the ferro-cement laminated masonry. At around 0.6% drift, wire meshes started to be ruptured in the inclined crack which leads to sudden drop in lateral resistance. At this stage, sliding at the joint of strengthened wall and top beam has been started and also shear crack formed at the top of tension column. At about 1.5% story drift, direct / punching shear failure at top of the tension column, as shown in Fig. 6(a), has also been observed which has been confirmed by recorded strain values of the tie. Loading has been stopped at the 1st cycle of negative 2% lateral drift, where the bottom reinforcement of compression column buckled which is followed by cover concrete spalling. The final crack pattern under lateral cyclic loading is shown in Fig. 6(a).

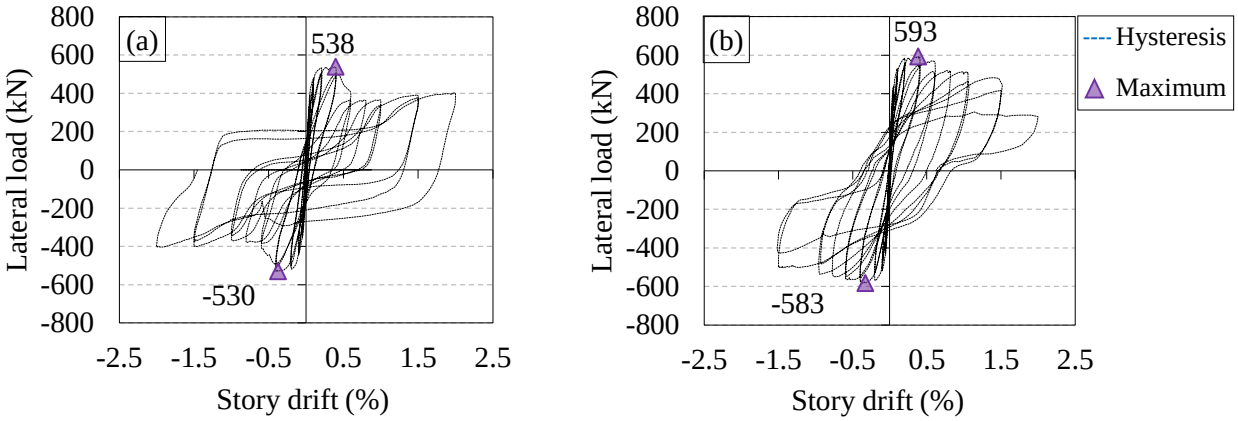

Fig. 5- Lateral load-story drift relationship of specimen (a) IM-FC-1, and (b) IM-FC-2

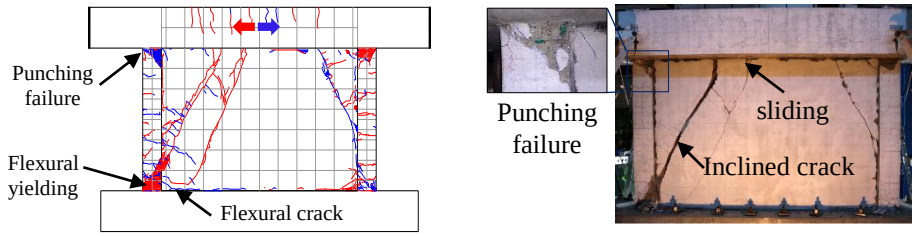

(a) Specimen IM-FC-1

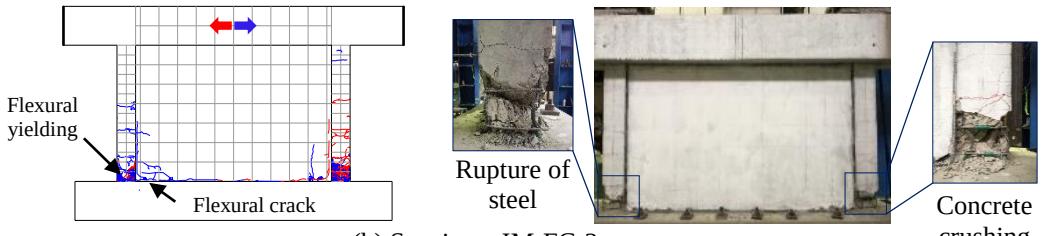

(b) Specimen IM-FC-2

Fig. 6- Crack pattern of specimen (a) IM-FC-1 and (b) IM-FC-2

3.1.2 IM-FC-2 (with higher wire mesh ratio i.e. 0.56%)

The hysteresis loops of IM-FC-2 is shown in Fig. 5(b). The response was also linear up to the formation of first crack on tension column at 0.05% lateral drift. The longitudinal reinforcements at the bottom of tension column experienced yielding at 0.1% story drift. At 0.1~0.2% story drift, flexural crack at the joint of wall and stub beam, as shown in Fig. 6(b), has also been observed. After that, the tension crack at the bottom of column gradually increased up to 3mm. At about 1% story drift, core concrete of compression column started to crush. Wire meshes at the bottom of the wall, which have been connected directly to beam through steel plate and bolt, started to be ruptured at about 1.5% story drift. Loading has been finished at the 1st cycle of negative 2% lateral drift, where three out of six main reinforcements of tension column ruptured. The final crack pattern under lateral cyclic loading is shown in Fig. 6(b).

3.2 Identification of failure mechanisms

Failure mode of structural wall, under lateral load, is mainly governed by shear, flexure or combination of the shear and flexure. To separate the contribution of flexure and shear in top displacement, the LVDTs attached on RC columns have been utilized to compute the flexural component of total story deformation. This is followed by the determination of shear deformation at a certain drift using Eq. (1).

$$\Delta_{total} = \Delta_{fl} + \Delta_{sh} \tag{1}$$

where, Δ_{total}, Δ_{fl}, Δ_{sh} refer to total, flexural and shear deformation, respectively at the center of top beam.

The obtained flexural and shear deformation in relation to the story drift are shown in Fig. 7(a)-(b). In specimen IM-FC-1, flexural contribution is relatively more at lower story drifts as shown in Fig. 7(a). At higher story drifts, tension column experienced direct punching shear failure following sliding at top joint which led to an increase in shear deformation. Another strengthened RC frame, namely IM-FC-2, experienced a flexure domination throughout course of the lateral drift as shown in Fig. 7(b). In other word, IM-FC-1 behaved as flexural wall at the drift until 0.4% and then failed in punching shear of column, but IM-FC-2 specimen behaved like a flexural wall for all story drifts (as shown in Fig. 8(a)). However, if bond at top construction joint fails, i.e. sliding, direct shear failure of tension column might happen as shown in Fig. 8(b).

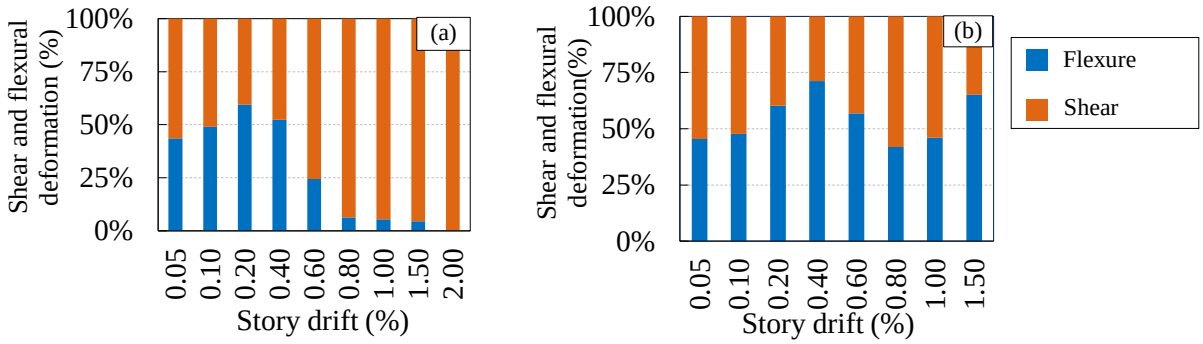

Fig.7- Shear and flexural contribution in story deformation of (a) IM-FC-1, and (b) IM-FC-2

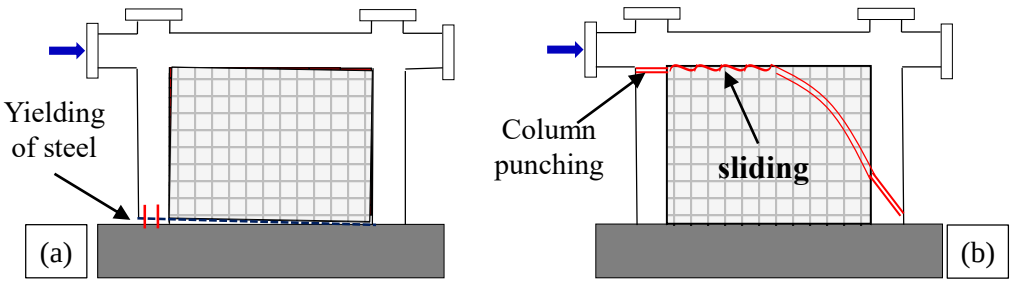

Fig. 8- (a) Flexural failure and (b) Column punching and joint failure of FC laminated specimens

3.3 Comparison of lateral behavior

The envelope curves of FC laminated masonry infilled RC frames are shown in Fig. 9. Comparing the peak resistance, it can be summarized that wire mesh ratio did not affect the lateral strength much because at peak resistance load transfer mechanism has been mainly governed by flexure for both specimens. Specimen with 0.16% mesh ratio, IM-FC-1, showed 25% capacity drop after peak resistance due to bond failure at top joint following by sliding. The specimen with 0.56% mesh ratio IM-FC-2, showed very gradual post peak declination which indicates a relatively ductile behavior.

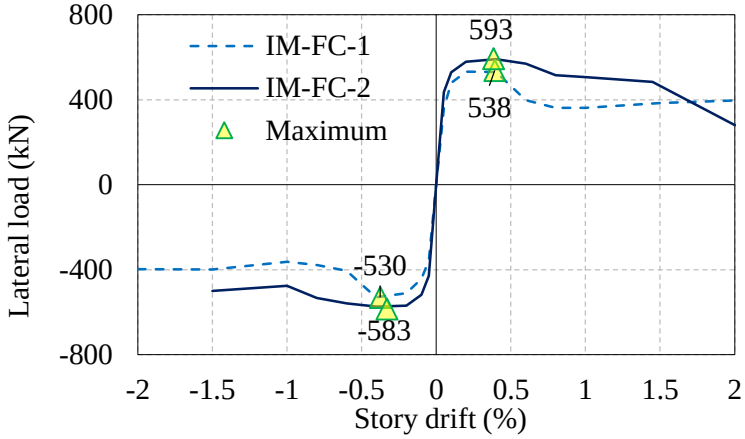

Fig. 9- Comparison of backbone curves

4. Possible failure modes

Generally, failure mode of masonry/concrete infilled RC frame depends on relative stiffness as well as strength of infill material compared to surrounding RC frame. In case of masonry infilled RC frame, infill masonry is generally the weakest part, therefore failure initiates on the masonry part. However, ferro-cement laminated infill masonry has higher stiffness and strength compared to infill masonry. Therefore, RC frame could be the weakest part and consequently can fail as observed in the current experimental program. Meanwhile, crushing or cracking of FC laminated infill masonry is also evident in literature. Kaya et al. [1] investigated FC laminated masonry infilled RC frame where, crushing due to diagonal compression is evident as shown in Fig. 10(a). In that study [1], 0.32% of wire mesh embedded mortar layer (of 7.9 MPa compressive strength) has been applied on infill masonry having compressive strength of 7.8MPa. One specimen, named Sp-5 of Kaya et al. [1] will be used in next section for strength evaluation of diagonal compression failure. In addition, diagonal cracking of strengthened masonry is also evident in a study by Seki et al. [2], as shown in Fig. 10(b). In other studies [3-6], failure has not been clearly identified.

Based on the current experimental observation and previous studies [1-2] four distinct failure modes, as shown in Fig. 11, have been identified. The lateral strength evaluation of Failure I, II and III are discussed in the following section.

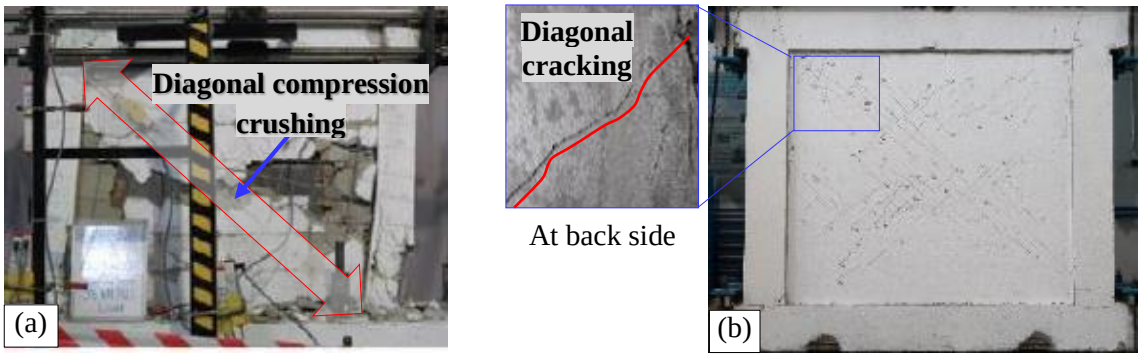

Fig. 10- (a) Diagonal compression [1] and (b) Diagonal cracking [2] of FC strengthened infilled masonry

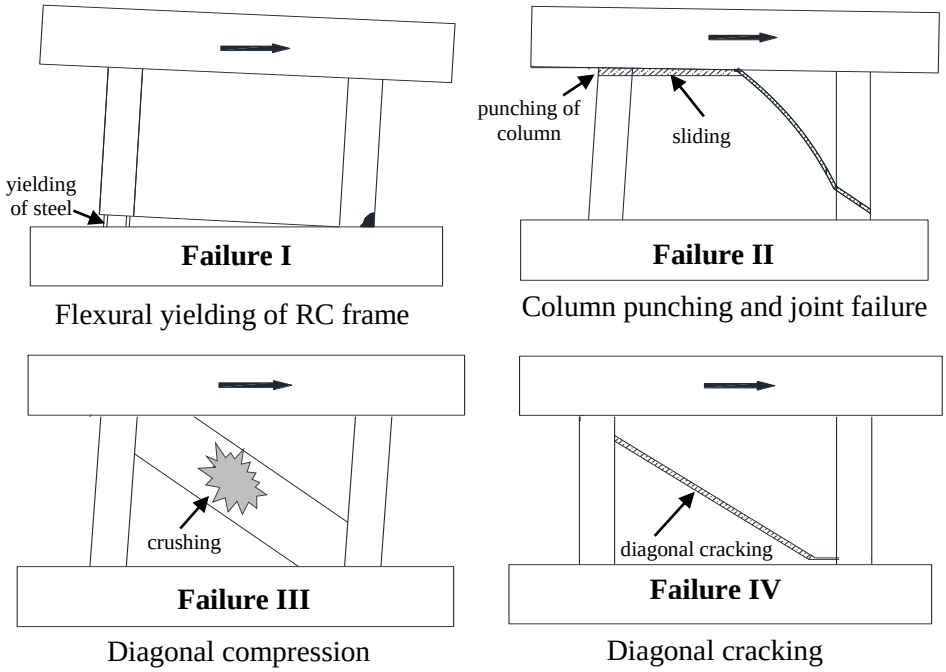

Fig. 11- All possible failure modes of ferro-cement laminated masonry infilled RC frame

5. Evaluation of failure mechanisms

In this section, capacity evaluation of Failure modes I, II and III are discussed in details and validated with current and past experimental study [1]. Failure mode IV has been discussed in authors' another study [10].

5.1 Failure I: Flexural yielding of RC frame

The lateral capacity at flexural yielding of RC frame (Q_1), as shown in Fig. 12(a), of the FC laminated masonry infill in RC frame has been computed from flexural theory, using Eq. (2) and Eq. (3). It is to be noted that, in ultimate moment calculation (Eq. 3) the contribution of wire meshes has been ignored because wire meshes have been connected at intervals with stub beam. Therefore, the lateral capacity is thought to be provided by the only RC frame.

$$Q_1 = {}^{M_u}/_{h_o} \tag{2}$$

$$M_u = a_t f_y l_c + 0.5 N l_c \tag{3}$$

where, M_u = ultimate moment capacity of RC frame; h_o = clear height of column; a_t = cross sectional area of column longitudinal reinforcements; f_y= yield strength of column longitudinal reinforcement; l_c = c/c distance of boundary columns, and N=axial load on RC columns.

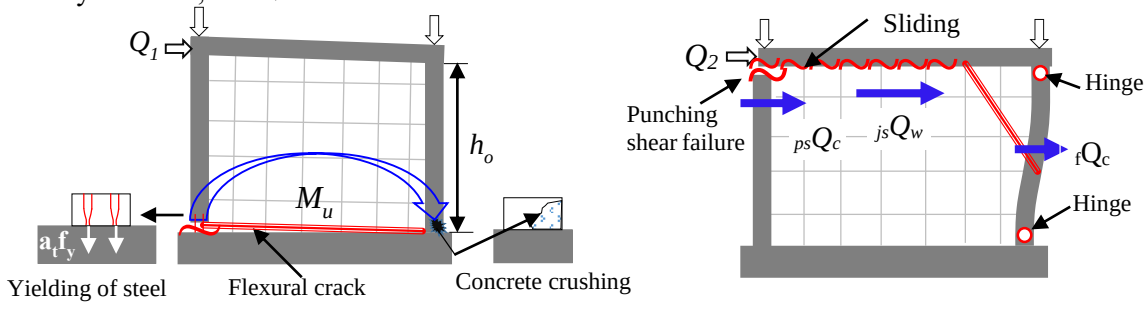

Fig. 12- Load transfer mechanism of (a) Flexural yielding of frame (Failure I) and (b) Column punching and joint failure (Failure II)

5.2 Failure II: Column punching and top joint failure

Free body diagram of FC strengthened masonry infilled RC frame after top construction joint failure and column punching is shown in Fig. 12(b), which actually occurred in specimen IM-FC-1 at higher story drifts. The total shear capacity (Q_2) can be evaluated by Eq. (4).

$$Q_2 = {}_{ps}Q_c + {}_{js}Q_w + {}_{f}Q_c \tag{4}$$

where, ${}_{ps}Q_c$ = punching shear resistance of tension column; ${}_{js}Q_w$ = shear resistance at top construction joint, and ${}_{f}Q_c$= flexural shear resistance of compression column.

Punching shear capacity (${}_{ps}Q_c$) of tension column, and lateral capacity of compression column (${}_{f}Q_c$) of RC column can be computed as per JBDPA [11] using Eq. (5) and Eq. (6), respectively. The source of joint shear capacity (${}_{js}Q_w$) could be the masonry joint mortar, mortar of FC layer and embedded wire meshes in FC layer. From the lateral behavior of specimen IM-FC-1, it is clear that initially shear strength is greater than flexural capacity (i.e. shear failure after flexural yielding) and the lateral resistance degraded 25% after occurring slippage at the top construction joint. This indicates that initially the bond between FC laminated masonry and soffit was working. Then, after slippage, wire meshes were working as dowel to provide residual capacity. Therefore, at initial stage, before any slippage at the interface of infill top and soffit, shear capacity can be considered as shear strength (cohesion) of mortar at interface. In initial bond capacity, wire mesh might have contribution in addition to mortar cohesion however, as a conservative approach wire mesh contribution has been ignored. After the occurrence of slippage wire mesh will be subjected to shearing force hence considered as the source of residual shear capacity at the interface. After slippage, friction might also work, however, has not been considered here for simplicity. The initial and residual joint shear capacity can be evaluated from Eq. (7) and Eq. (8), respectively.

$${}_{ps}Q_c = K_{\min}\tau_o bD \tag{5}$$

$${}_{f}Q_c = \frac{2M_c}{h_o} \tag{6}$$

$${}_{js}Q_{wi} = \tau_{mas} l_w t_{mas} + \tau_{mor,FC} l_w n_s t_{FC} \tag{7}$$

$${}_{js}Q_{wr} = \sum a_{wm}\, \tau_{y,wm} \tag{8}$$

where, K_{min} = 0.34/(0.52+a/D); a= shear span = D/3; τ_o = shear strength of tension column; b and D = width and depth of column; M_c= ultimate moment capacity of column; h_o= clear height of column; ${}_{js}Q_{wi}$ = initial shear capacity at joint; ${}_{js}Q_{wr}$ = residual shear capacity at joint; τ_{mas} , $\tau_{mor,FC}$ = shear strength (cohesion) of mortar in masonry joint and ferro-cement; l_w = length of infill; t_{mas} , t_{FC} = thickness of masonry wall and FC layer; n_s = number of FC surface; a_{wm} = cross sectional area of wire mesh; $\tau_{y,wm}$ = shear strength of wire mesh ($f_{y,wm}$ /√3). It is to be noted that cohesion capacity of mortar, for both masonry and FC layer, has been considered as 0.17√f_{mor} (where f_{mor} =compressive strength of mortar), which has been recommended by Namaan 2000 [12], and Mander and Nair 1994 [13] as shear strength of FC. The yield strength of wire mesh, ($f_{y,wm}$ = 0.925*$f_{u,wm}$) has been considered as per AS/NZS [14].

5.3 Failure III: Diagonal compression failure

In diagonal compression failure, infilled part (masonry and FC layer) has been considered to behave similar to a diagonal strut, as shown in Fig. 13, that would fail in compression. In addition, flexural hinges would form at the top and bottom of surrounding RC columns. The lateral strength (Q_3) can be evaluated by using Eq. (9).

$$Q_3 = 2\,{}_{f}Q_c + \left(0.5 f_{m,90} W_s t_{mas} + 0.5 f_{mor,FC} W_s n_s t_{FC}\right) Cos\theta \tag{9}$$

where, ${}_{f}Q_c$= flexural shear resistance of RC column; $f_{m,90}$ = expected prism compressive strength of masonry in horizontal direction (= 0.5 x masonry prism compressive strength, f_m); $f_{mor,FC}$ = FC mortar compressive strength; W_s = strut width of FC laminated masonry; t_{mas}, t_{FC} = thickness of masonry and FC mortar layer; n_s = number of surface retrofitted with FC, and θ = inclination of loaded diagonal with horizontal.

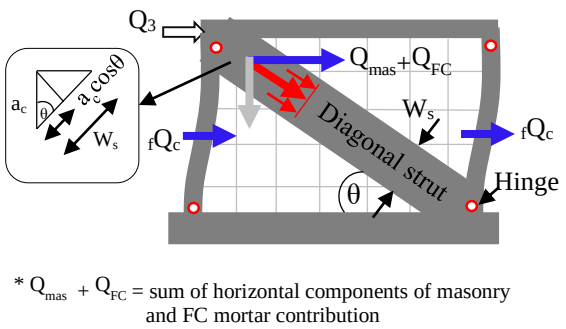

* Q_{mas} + Q_{FC} = sum of horizontal components of masonry and FC mortar contribution

Fig. 13- Load transfer mechanism of diagonal compression failure

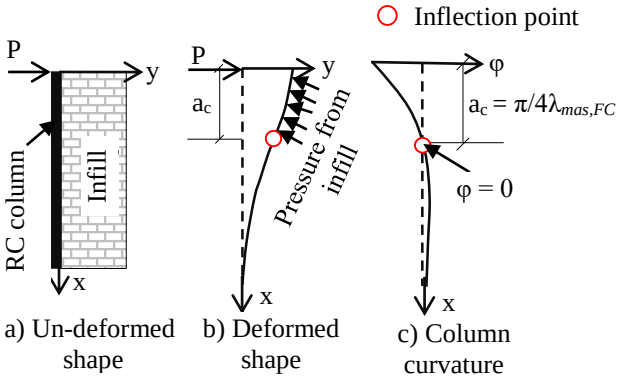

Fig. 14- Effective contact between infill and RC column.

In Eq. (9), flexural capacity of RC column ($_fQ_c$) can be evaluated using Eq. (6). Other parameters, except diagonal strut width (W_s), are mostly related to masonry and FC materials and geometry. Therefore, diagonal strut width of FC laminated masonry is focused herein. For masonry or concrete infilled RC frame, strut width depends on the relative rigidity of infill material in comparison to surrounding RC column [15]. Under lateral loading, RC column is considered as a beam element resting on infill material, as shown in Fig.14(a), where infill material would act a foundation of the loaded beam element. The lateral deflection (y) and curvature (φ) of the RC column could be evaluated considering it is analogous to a beam on elastic foundation. According to the theory of elasticity, general solution of beam deflection (y) resting on an elastic foundation can be expressed by Eq. (10) [16], where, relative rigidity (λ) of foundation with respect to beam has been defined as Eq. (11).

$$y = \frac{P\lambda}{2bk_o} e^{-\lambda x}(sin\lambda x + cos\lambda x) \tag{10}$$

$$\lambda = \sqrt[4]{\frac{bk_o}{4EI}} \tag{11}$$

where, P =lateral load; b = foundation thickness; k_o= modulus of foundation i.e. pressure required to get unit deflection of foundation; E = Young's modulus of beam element i.e. concrete, and I = moment of inertia of beam element i.e. column.

Considering the flexural rigidity of RC column (EI) and modulus of FC laminated masonry strut following relative rigidity factor ($\lambda_{mas\text{-}FC}$) for FC laminated masonry is defined here as Eq. (12).

$$\lambda_{mas-FC} = \sqrt[4]{\frac{(E_{mas}t_{mas}+E_{FC}n_s t_{FC})\,cos^2\theta}{4E_C I_c d_m}} \tag{12}$$

where, E_c, E_{mas}, E_{FC} = young's modulus of concrete, masonry, FC mortar; t_{mas}, t_{FC} = thickness of masonry, FC mortar layer; n_s = number of surface retrofitted with FC; I_c = moment of inertia of RC column; d_m = diagonal length of infill panel, and θ = inclination of loaded diagonal with horizontal.

It is evident from the column deflection shape, as shown in Fig. 14(b), that the lower portion of RC column exhibits flexure deflection whereas the deflection mode of upper part is changed from flexural shape due to presence of infill masonry, which actually causes the separation between masonry and RC frame. Based on the deflection shape, it has been considered that the infill panel of the upper part of inflection point is attached with RC frame effectively and considered as contact length (a_c) of diagonal strut. The height of inflection point i.e. effective length (a_c) has been evaluated from the condition of zero curvature at inflection point, as shown in Fig. 14(c), using Eq. (13). The curvature of RC column, as shown in Fig. 14(c), has been determined from the second derivative of column deflection (y). Subsequently, width of the diagonal strut (W_s) has been calculated by using Eq. (14), in reference to Fig. 13.

$$a_c = \frac{\pi}{4\lambda_{mas-FC}} \quad (13)$$

$$W_s = 2a_c cos\theta \quad (14)$$

where, a_c =effective contact length; W_s = strut width; $\lambda_{mas\text{-}FC}$ = relative rigidity factor for FC laminated masonry, and θ = inclination of loaded diagonal with horizontal.

6. Validation of capacity evaluation

In this section, capacity prediction models of Failure mode I (flexural yielding of RC frame) and Failure mode II (column punching and top joint failure) are validated using current experimental program. However, the capacity of Failure mode III (diagonal compression failure) is validated with the specimen Sp-5 from Kaya et al. [1] because this particular failure did not happen in the current experimental program. All the calculated capacities are given in Table 3 and also shown in Fig. 15(a) – (c).

Failure mode I (flexural yielding of RC frame) is investigated using experimental observation of the specimen IM-FC-1 and IM-FC-2 as shown in Fig.15(a). The proposed evaluation by Eq. (2) showed good estimation of the experimental capacities, as shown in Table 3 and Fig.15(a) and the average calculated to experimental capacity ratio is 0.93 and 0.84 for specimen IM-FC-1 and IM-FC-2, respectively. It indicates that the calculated flexural capacity (using Eq. (2)) without considering wire mesh can give good and fairly conservative approximation of lateral load capacity.

The post peak response of specimen IM-FC-1 has been governed by the Failure mode II (column punching and joint failure) hence the residual shear capacity can be evaluated using Eq. (4). The calculated component capacities of RC frame and ferro-cement at the post peak stage of column punching and joint failure are shown in Fig. 15(b).

Table 3- Lateral capacity of specimens

Lateral capacity (kN)		Current study		Kaya et al. (2018) [1]
		IM-FC-1	IM-FC-2	Sp-5
Experimental	Peak (avg.)	534	588	155
	Residual (avg.)	373	-	-
Flexural capacity, Q_1 [Eq. (2)]		494	494	212
Initial shear capacity, Q_2		487	485	174
Residual shear capacity, $Q_{2,residual}$		278	481	-
Diagonal compression capacity, Q_3 [Eq. (9)]		646	683	109

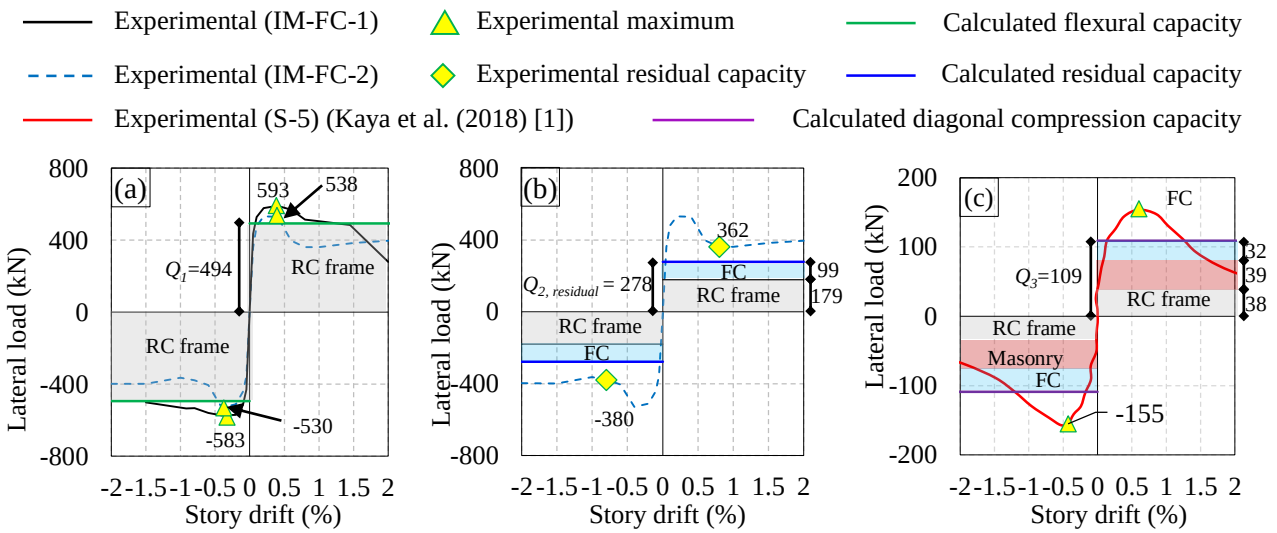

Fig. 15- Calculated capacity of (a) Failure I (flexural yielding of RC frame) (b) Failure II (column punching and joint failure) and (c) Failure III (diagonal compression failure)

The estimated residual capacity is 278kN, with average calculated to experimental capacity ratio of 0.75. It indicates a relatively conservative estimation residual shear resistance which could be attributed to the friction at the top joint interface which has not been considered.

Failure mode III (diagonal compression failure) is validated using specimen Sp-5 from the experimental program from other study by Kaya et al. [1]. The calculated component capacities are shown in Fig. 15(c). The average calculated to experimental capacity ratio is 0.7 for specimen Sp-5 [1] which indicates a conservative estimation of experimental result.

7. Conclusions

In this study, an experimental investigation has been conducted on the lateral behavior of two ferro-cement laminated infilled RC frame with varying wire mesh steel area ratio. The following conclusions can be drawn from this study-

a. The observed failure mechanism of the studied ferro-cement laminated specimens, with 0.16% and 0.56% mesh ratio, were flexural yielding of RC frame, at the peak resistance, like structural wall which is not identified in literature.

b. Since, ferro-cement laminated masonry walls did not participate in load transfer mechanism of flexural yielding of RC frame directly therefore wire mesh ratio, 0.16% and 0.56%, did not strongly affect the lateral capacity of ferro-cement strengthened masonry infilled RC frame.

c. Based on current study and past studies, four distinct possible failure modes have been identified. Among four, lateral capacity estimation method for three failure modes have been proposed and verified with fair agreement with current and previous experimental results.

Above conclusions are based on limited number of experimental test specimens, therefore further experimental studies are required to apply the proposed capacity prediction procedure in evaluation or design purpose.

8. Acknowledgement

This research is supported by SATREPS project "Technical Development to Upgrade Structural Integrity of Buildings in Densely Populated Urban Areas and its Strategic Implementation towards Resilient Cities (TSUIB)" (principle investigators: Prof. Yoshiaki Nakano, U. Tokyo and Mr. Mohammad Shamim Akhter, HBRI, Bangladesh) and JSPS KAKENHI Grant Number JP18H01578 (Principal investigator: Prof. Masaki Maeda, Tohoku University).

9. References

[1] Kaya F, Tekeli H, Anil Ö (2018): Experimental behavior of strengthening of masonry infilled reinforced concrete frames by adding rebar‐reinforced stucco. *Structural Concrete*, **19** (6), 1792-1805.
[2] Seki M, Popa V, Lozinca E, Dutu A, Papurcu A (2018): Experimental study on retrofit technologies for RC frames with infilled brick masonry walls in developing countries. *Proceedings of the 16th ECEE*.
[3] Demirel IO, Yakut A, Binici B, Canbay E (2015): An Experimental Investigation of Infill Behaviour in RC Frames. *10th Pacific Conference on Earthquake Engineering Building an Earthquake-Resilient Pacific* (pp. 6-8).
[4] Altın S, Anıl Ö, Kopraman Y, Belgin Ç (2010): Strengthening masonry infill walls with reinforced plaster. *Proceedings of the Institution of Civil Engineers-Structures and Buildings*, **163**(5), 331-342.
[5] Calvi GM, Bolognini D (2001): Seismic response of reinforced concrete frames infilled with weakly reinforced masonry panels. *Journal of Earthquake Engineering*, **5**(02), 153-185.
[6] Žarnić R, Tomaževič M (1985): Study of the behaviour of masonry infilled reinforced concrete frames subjected to seismic loading.
[7] Japanese Industrial Standards (2010): Japanese Standard Association.
[8] ACI 549 1R-93 (1993): *Guide for the Design, Construction and Repair of Ferro-cement* (Reapproved 1999).
[9] American Society of Testing and Materials (2011): *Standard test method for compressive strength of masonry prisms*.
[10] Sen D, Lamsal J, Dutu A, Alwashali H, Seki M, Maeda M (2020): Experimental study on Ferro-cement retrofit for RC frame with infilled brick masonry wall. *17th World Conference on Earthquake Engineering*, Sendai, Japan.
[11] *Standard for seismic evaluation of existing concrete* (2001): Japan Building Disaster Prevention Association.
[12] Naaman AE (2000): *Ferrocement and laminated cementitious composites* (Vol. 3000). Ann Arbor: Techno press.
[13] Mander JB, Nair B (1994): Seismic resistance of brick-infilled steel frames with and without retrofit. *Masonry Journal*, **12**(2), 24 - 37.
[14] AS/NZS 4671 (2001): *Steel reinforcing materials*.
[15] Smith BS (1966): Behavior of square infilled frames. *Journal of the Structural Division*, **92**(1), 381-404, 1966.
[16] Hetenyi M (1946): *Beams on elastic foundation*. The University of Michigan press, London.

